



OPEN

Microwaves induced epitaxial growth of urchin like MIL-53(Al) crystals on ceramic supports

Limor Ben Neon¹, Martin Drobek¹, Mikhael Bechelany^{1,2}, Bertrand Rebiere³ & Anne Julbe^{1✉}

Shaping Metal–Organic Frameworks (MOFs) poses a significant challenge for their widespread application on a large scale. In particular, a precise control over crystal orientation and arrangement on substrates are expected to provide exiting opportunities for novel materials with customized characteristics and enhanced performance in catalysis, gas storage, sensing, optics and electronics. Here we demonstrated for the first time that microwave irradiation can induce well controlled epitaxial growth of urchin-like MIL-53(Al) crystals via the hydrothermal conversion of Atomic Layer Deposition alumina layers on SiC foams. The resulting large, ordered crystals feature specific size, homogeneity, dispersion, and quantity that strongly correlate with the nature of the ceramic support and its ability to absorb microwaves. Furthermore, the supported MIL-53(Al) urchins were considered as templates for generating nanostructured alumina fibers on SiC foams, providing attractive catalyst carriers with high specific surface areas.

Metal–organic-frameworks (MOFs) are porous structures built from metal ions coordinated with organic ligands¹. Due to their tunable structure, flexibility, high specific surface and porosity, MOFs have emerged as valuable candidates for gas storage, membrane separation, environmental remediation, sensors, drug delivery, catalysis and other applications^{1,2}. Among the best known and most studied MOFs, special attention is paid to MIL-53 due to its unique structure, built from metal ions (e.g. Cr, Fe or Al) octahedrally coordinated to two hydroxyl groups and four oxygen atoms of the deprotonated terephthalic acid ligand (TA). Indeed, MIL-53(Al) is proved to be a promising material for gas separation (i.e. CH₄/N₂)³, gas sensing (CO₂)², VOC adsorption⁴, desalination of dye solutions⁵ or catalysis². However, despite the wide-range of potential applications, their industrial use is still rather scarce. In fact, long synthesis times and the difficulty of shaping MOFs into robust and mechanically stable macroscopic bodies such as pellets, beads, granules etc. limit their use on larger scales¹. Generally, MOFs are obtained in the form of microcrystalline powders and their pulverous nature complicates their industrial application since it can lead to clogging of pipelines and loss of active material. Moreover, powders pose also storage and transport difficulties and can cause health issues during handling. In addition to their shaping as self-supported materials, an efficient growth/dispersion of MOFs on macroscopic substrates such as membrane supports, fibers and foams is required. This is a crucial step for the practical implementation of MOFs on an industrial scale.

In this regard, one can consider either the deposition/dispersion of the already synthesized MOF powder on an appropriate support (e.g. polymer matrix⁶) or its direct growth on the support itself. For the latter, the conversion of oxide-to-MOF appears to be a very promising strategy to obtain hierarchically structured MOFs with well-organized polycrystalline structures⁷. In fact, the ceramic's surface is serving as a metal-ion source reacting with organic linkers to form MOF structures directly on the support as demonstrated elsewhere^{8,9}.

However, long synthesis times, high energy consumption and excessive use of organic solvents inducing toxicity and environmental pollution limit the industrial implementation of such systems. Thereby, to make this process eco-friendly and more attractive for manufacturers, the use of microwaves (MW) appears to be an ideal solution. Indeed, MWs are known for their beneficial impact on reaction kinetics, enabling shorter reaction times and lower reaction temperatures^{10,11}. In addition, MWs could favor specific reaction pathways which are not achievable with conventional heating, generate less waste, induce high reaction yields and phase purity in very short reaction times^{10,12}. Heating under MW irradiation is induced by the capacity of the solvent, precursors

¹Institut Européen des Membranes (IEM), Univ Montpellier, CNRS, ENSCM, Place Eugène Bataillon, 34095 Montpellier, France. ²Gulf University for Science and Technology, GUST, Sabah Al-Salem, Kuwait. ³UAR Plateforme d'Analyses et Caractérisations (PAC) Chimie Balard Montpellier, Univ Montpellier, CNRS, ENSCM, Place Eugène Bataillon, 34095 Montpellier, France. ✉email: anne.julbe@umontpellier.fr

and/or the solid support to transform the absorbed MWs into thermal energy. This capacity is reflected by the dielectric loss (ϵ'') which is specific to each solvent and solid¹².

Water and the semiconductor SiC exhibit high dielectric losses. Combining both compounds for the metal oxide-to-MOF conversion reaction under MW-assisted heating thus appears as an economical and environmental friendly strategy to grow MOFs on ceramic supports.

Water is a green solvent acting as a moderate thermal dissipator¹³ under MW irradiation. It enables fast and uniform heating of the reaction medium compared to conventional heating methods. When the boiling point of water is exceeded, the hydrogen bonds between water molecules break and the water becomes less polar, behaving more like an “organic solvent”. This ability improves the dissolution of organic linkers, which are usually preferentially soluble in organic solvents. Additionally, SiC is well known for its high thermal conductivity under MW irradiation ($\epsilon'' \sim 28$), leading to rapid and homogeneous heat dissipation on its surface¹⁴. Given this specific property of SiC and its commercial availability on a large scale with relatively low cost, this material can be considered as a very attractive support for the *in-situ* growth of MOF polycrystals under MW irradiation. Finally, since the solid and liquid phases are affected by MW irradiation, their mutual interface can be easily polarized, thus forming a hydrothermal micro-environment promoting high reaction efficiency¹⁵. Such MW-derived interfacial effects might favor the growth of uniform MOF crystals distributed homogeneously on the SiC surface.

Based on this premise, and in order to apply the oxide-to-MOF conversion strategy, the SiC support must be coated with a metal oxide layer that will serve as the only metal source for the selected MOF. For this purpose, Atomic Layer Deposition (ALD) is a particularly suitable technique, producing uniform and conformal coatings with controlled thickness and composition, even on supports with complex geometries such as SiC foams. This vapor phase deposition method does not require any solvent and consumes a minimum quantity of metal precursor. The possibility of transforming ALD metal-oxide layers into MOFs in the presence of organic ligands and organic solvents has already been reported by the authors^{7,16–18}. For example, ALD coatings such as ZnO and Al₂O₃ were easily converted to ZIF-8 and NH₂-MIL-53(Al), respectively^{16–18}.

Based on this expertise and the attractive behavior of water and SiC under MW irradiation, we hereby report for the first time a green and eco-friendly MW-assisted approach to grow directly MIL-53(Al) crystals on SiC foams. The strategy consists first in coating the SiC foams with an alumina (Al₂O₃) layer by ALD. This layer is then converted to MIL-53(Al) via a MW-assisted hydrothermal reaction in the presence of an aqueous solution of the selected organic ligand (e.g. terephthalic acid for MIL-53(Al)). After synthesis, the ligand solution could be recovered, filtered and recycled for subsequent reaction runs. This option can thus have a positive environmental and economic impact on a large scale, especially when taking into account also the reduction of energy consumption and synthesis time. In addition, this work demonstrates that the reaction conversion under MW irradiation significantly impacts on the growth, orientation, shape and distribution of MIL-53(Al) crystals formed on the SiC support.

Experimental Synthesis

Conditioning of ceramic foams

Ceramic foams composed of SiC with 10 PPI (pores per inches) were supplied by EPMF-France. These industrial foams are produced at large scale by FOSECO-VESUVIUS with the reference SEDEX-SiC-10 PPI. Before use, the SiC foams were cut into 0.5 × 1.5 × 1.5 cm large pieces with a diamond cut-off-wheel MOD20 (203 mm dia. × 0.6 mm × 20 mm dia., Struers). The ceramic particles released during this cutting operation were immediately flushed out using a strong flow of tap water to avoid any clogging of the foam pores. Afterwards the pieces were washed thoroughly with Milli-Q water and finally ethanol (≥ 99.8%, Sigma Aldrich). After drying at 120 °C overnight, the foams were thermally treated in stagnant, ambient air at 500 °C for 4 h (5 °C/min) using a muffle furnace (Nabertherm L3/11/B170).

Atomic Layer Deposition (ALD) of Al₂O₃

A home-made ALD experimental *set-up* (Figure S1) was used to deposit Al₂O₃ thin layers on the conditioned SiC foams. ALD was carried out at 100 °C using sequential exposures of trimethylaluminum (TMA, 97%, Sigma Aldrich) and deionized water, separated by a purge of dry argon (≥ 99.999%, from Linde Electronics) with a flow rate of 100 sccm. The deposition protocol was as follows: (a) 0.4 s pulse TMA, 30 s exposure and 40 s purge with dry Ar; (b) 2 s pulse of H₂O, 30 s of exposure, and 40 s purge with dry Ar. 250 cycles were carried out to obtain an average coating thickness of 50 nm (thickness verified by ellipsometry on Si-wafer). Each foam was weighed (KERN ANT-220-5DNM balance) before and after ALD to estimate the amount of deposited alumina. The alumina-coated SiC foams were referenced as ALD-Al₂O₃.

Metal oxide-to-MOF conversion

The thin ALD-Al₂O₃ layer on SiC foams was converted to MIL-53(Al) using a MW-assisted hydrothermal synthesis protocol. Briefly, 0.4 g of terephthalic acid (TA) (98%, Merck) were dissolved in 40 mL of Milli-Q water (1 wt% TA solution). This reaction solution and the alumina-coated foams were transferred to a Teflon™ pressure vessel and heated for 1.5 h at 220 °C (P = 600W, 44 °C/min) using a Microsynth Milestone microwave oven equipped with a HPR 1000/10 rotor. After the reaction, the ceramic foams decorated with MOF labeled MIL-53@SiC, were retrieved from the Teflon vessel and washed first with Milli-Q water, then with DMF (N,N-Dimethylformamide, 99.8%, SigmaAldrich) and finally again with Milli-Q water to remove DMF. Eventually, the samples were dried at 120 °C for 12 h in air.

For the sake of comparison, ALD-Al₂O₃ on SiC was also converted to MIL-53(Al) using conventional heating for the hydrothermal reaction step. Herein, the same heating temperature and ligand concentration were used as

for the MW-assisted hydrothermal approach. The synthesis protocol was inspired by the work of Yi Liu et al.¹⁹ in which MIL-53(Al) powder was synthesized under classical hydrothermal conditions. Briefly, the SiC foams coated with ALD- Al_2O_3 were introduced into 1 wt% TA solution in an autoclave and heated in a conventional oven for 72 h at 220 °C. The supports were washed and dried as previously described. The as-prepared samples were labeled MIL-53@SiC-CONV.

All dried samples were weighed before and after MOF synthesis to estimate the amount of MIL-53(Al) deposited on ceramic foams.

Morphology, microstructure and elemental analysis

The surface morphology of pristine SiC and MOF-modified foams MIL-53@SiC and MIL-53@SiC-CONV was examined by Scanning Electron Microscopy (FESEM, HITACHI S-4800). The dimensions of grown MOF crystals were measured using an image processing program (Imagej2x). The elemental distribution of Al, Si, O and C was determined by Energy Dispersive X-ray Spectroscopy (EDX) using a Zeiss sigma 300 SEM equipped with an Oxford Instruments X-Max^N SDD detector. The SiC-based samples were metallized with platinum. Raman spectroscopy was used to confirm the presence of MIL-53(Al) on the surface of SiC foams. A HORIBA Jobin LabRAM HR800UV Raman spectrometer ($\lambda = 660$ nm, 1800 g mm^{-1} grating) equipped with a Leica PL Fluotar $\times 50$ objective ($\text{NA} = 0.55$) was used.

The porous structure of the supported MIL-53(Al) materials has been investigated by N_2 physisorption experiments. Samples were first outgassed under vacuum at 150 °C for 12 h and N_2 adsorption/desorption isotherms were recorded with a Micromeritics ASAP 2020 equipment. The specific surface area (S_{BET}) was calculated by the multipoint Brunauer–Emmett–Teller (BET) method. The total pore volume (V_p) was evaluated at a P/P_0 close to 0.995.

Mechanical stability of MOF crystals on ceramic foams

Since the designed system is intended to be applied in fluid filtration or continuous flow catalysis, a good adhesion of MIL-53(Al) to ceramic foams is of utmost importance. Sonication is a simple, quick, and reliable method used to test the adhesion of thin films on corrugated supports, for which standard adhesion tests as scratch-tape tests are not applicable. It involves immersing the coated substrate in a liquid medium and applying ultrasonic waves. High-frequency vibrations create intense agitation in the liquid which can challenge the adhesion of the film. This procedure is classically used by the authors and other groups for evaluating the durability and robustness of supported ceramic films and membranes^{20,21}. To simulate mechanical stress on foam samples, sonication experiments were conducted in ethanol using Fisher Bioblock 86480 sonicator with an applied power of 345 W for 15 and 60 min. Typically, 0.25 g of MIL-53@SiC were introduced into a 50 mL beaker containing 25 mL ethanol. Aluminum concentration [Al] was determined via EDX to evaluate any eventual loss of MIL-53(Al) during sonication. Moreover, SEM observations were conducted before and after sonication tests to visualize any change in the crystal dispersion and morphology.

Results and discussion

Metal oxide-to-MIL-53(Al) conversion of ALD-alumina coated SiC foams

The conversion of Al_2O_3 layers deposited by ALD on pristine SiC foams (Fig. 1a) into MIL-53(Al) resulted in the formation of large, rectangular crystals as observed by SEM (Fig. 1b,c). Indeed, the surface of SiC foam is uniformly covered with MOF crystals forming a unidirectional urchin-like pattern. We note an average MIL-53(Al) crystal size of $2.5 \pm 0.8 \mu\text{m} \times 0.5 \pm 0.2 \mu\text{m}$. Moreover, the crystal length of MIL-53(Al) is rather constant, around $\sim 2.0 \mu\text{m}$ (Fig. 1d). Thus, the upwards growth of MIL-53(Al) crystals in the presence of MWs (i.e. in the direction of their length) appears to be homogeneous on SiC support. The nature of the MOF material was confirmed by Raman spectroscopy due to the observed characteristic vibration bands of MIL-53(Al) in the range 800–1800 cm^{-1} (Figure S2). To the author's knowledge, such large MOF crystals presenting this type of urchin-like morphology, well-ordered and anchored to the surface of a ceramic support have never been reported in the literature.

EDX mapping (Figure S3) is evidencing the uniform distribution of MOF crystals on the surface of SiC foam. Moreover, the latter showed that carbon and oxygen atoms present in the MIL-53(Al) framework were solely located on the ceramic foams' surface, confirming virtually zero growth of MOF crystals in the bulk of the supporting material.

Compared to the ordered urchin structure of MIL-53(Al) formed by alumina conversion under MW irradiation (i.e., MIL-53@SiC), conventional heating generates entangled and disorganized nanorods (average diameter $\sim 0.20 \mu\text{m}$) when applying the same synthesis temperature and ligand concentration (Fig. 2). In addition, a significant difference in support weight increase was noticed between the two samples after MOF growth: 6.5 wt% and 9.1 wt% for MIL-53@SiC-CONV and MIL-53@SiC respectively (Table 1). Thus, as expected, higher conversion rates of ALD alumina to MIL-53(Al) were therefore achieved via MW heating. However, the morphological effects associated to the heating method do not seem to impact on the specific surface area and pore volume of the MOF. Indeed, the S_{BET} values determined for MIL-53@SiC and MIL-53@SiC-CONV are very similar (80 and 77 m^2/g , respectively—Table 1).

Hence based on these observations one would question which concomitant phenomena are occurring in the presence of MWs and are inducing the particular observed morphology of MIL-53(Al) and its epitaxial growth. Indeed, as mentioned in the beginning SiC is an excellent thermal dissipater under MW irradiation^{14,22}. Additionally to this property, SiC is benefitting from its native silica layer rich in hydroxyl groups necessary for the germination process of MOF(Al) on the SiC support²³. Herein a synergistic effect of these two characteristics

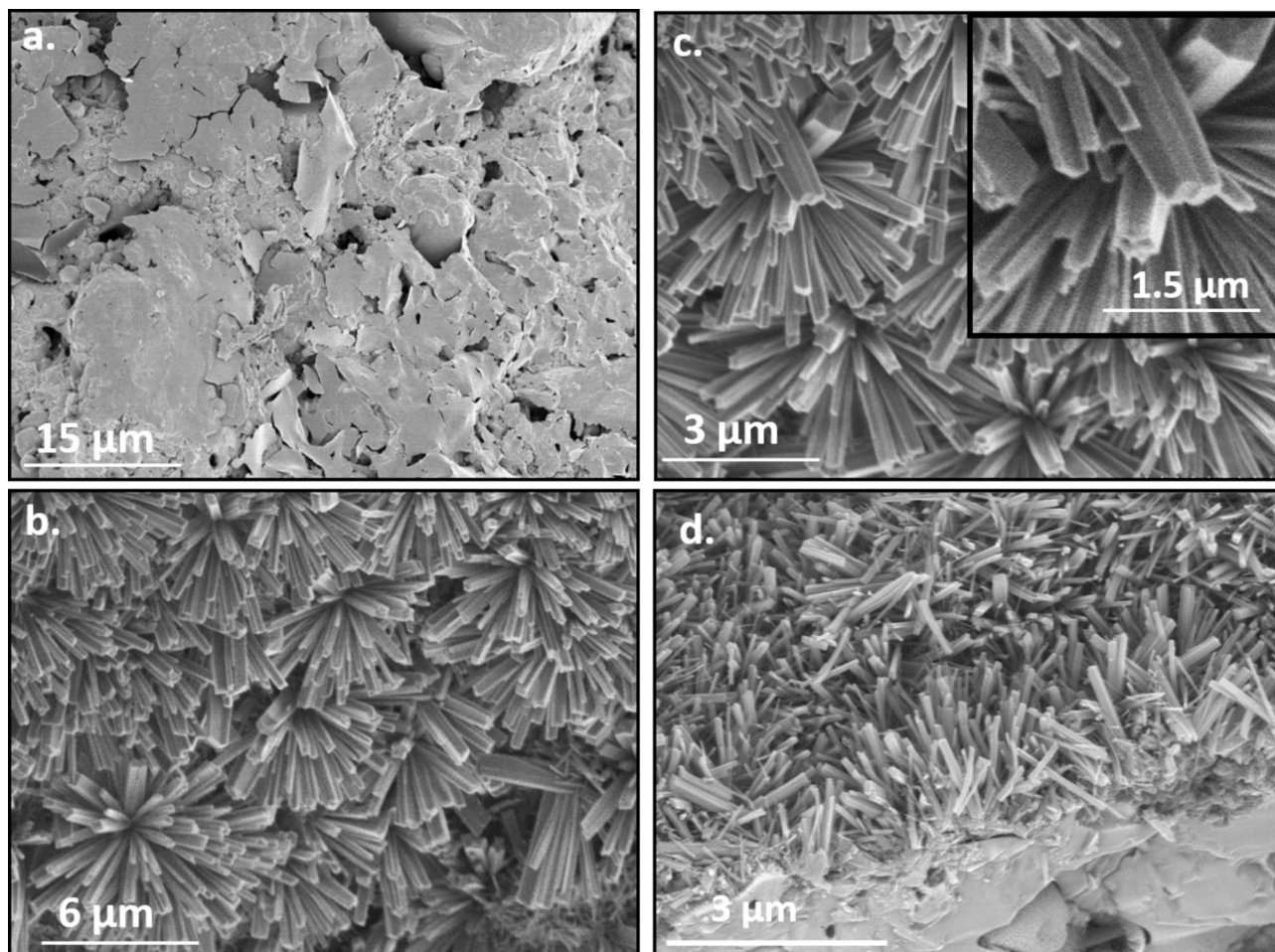


Fig. 1. SEM images of pristine SiC (a) foams; MIL-53(Al) urchin-like crystals grown on SiC foam (b,c) and its cross-section (d) by MW-assisted hydrothermal conversion of a thin ALD-alumina layer.

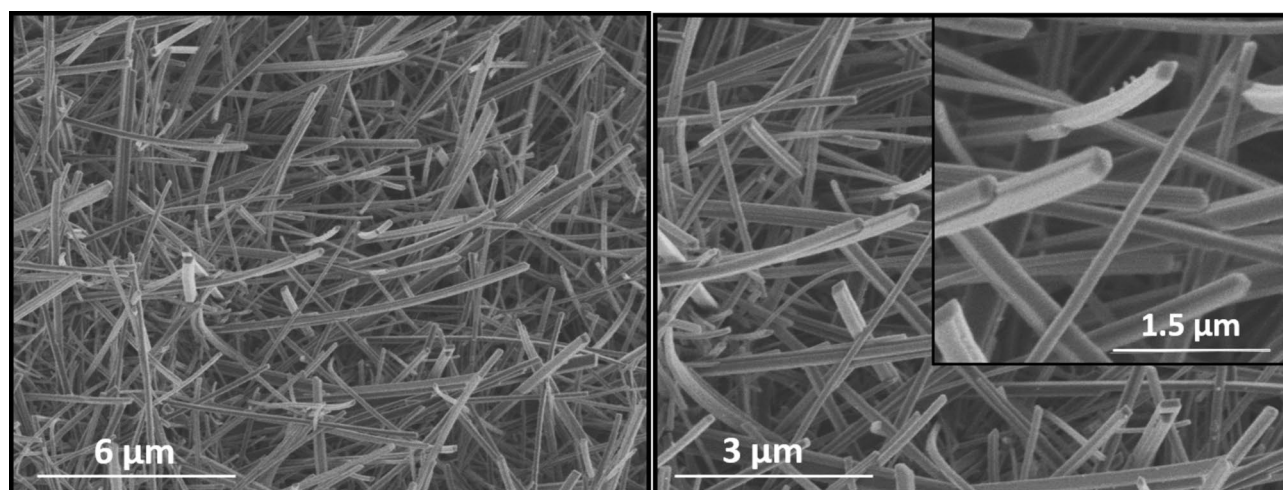


Fig. 2. SEM images of MIL-53@SiC-CONV synthesized via the hydrothermal conversion under conventional heating of a thin ALD-alumina top layer.

Sample	Δm (wt%) ^a	S_{BET} (m ² /g)	V_p (cm ³ /g)	S_{BET} (MIL-53(Al)) (m ² /g)	V_p (MIL-53(Al)) (cm ³ /g)
MIL-53@SiC	9.1	7	0.019	80	0.200
MIL-53@SiC-CONV	6.5	5	0.010	77	0.154

Table 1. Textural characteristics measured for MIL-53(Al) grown on SiC foams and extrapolated to the MIL-53(Al) material- Values of S_{BET} and pore volume (V_p) were attributed to the sole contribution of the MOF material (An error of ~10% is estimated on the S_{BET} , V_p). ^a $\Delta m = m_{(\text{sample after conversion})} - m_{(\text{pristine foam})}$.

needs to be considered since it could favor the creation of “anchoring sites” for MIL-53(Al) nuclei, leading to a uniform distribution of MIL-53(Al) crystals on SiC surface.

Besides, since the SiC-foam surface is expected to be heated more homogeneously during the reaction under MW irradiation due to high dielectric loss constant (Table S1), it enables a better control of crystal growth. Yet, it does not explain the formation of epitaxially grown urchins.

Therefore, one can question the role of ALD- Al_2O_3 . The thin ALD- Al_2O_3 layer is amorphous, rich in hydroxyl groups and very reactive. In the work of Kim et al.²⁴ it was demonstrated that the epitaxial growth of MIL-53(Al) on metal particles seemed to depend strongly on the competition between coordination and dissolution kinetics. The later was favored at synthesis temperatures exceeding 200 °C, and subsequently induced the growth of 1D oriented MOF(Al) crystals. Since ALD-alumina is strongly reactive the dissolution of Al^{3+} at 220 °C might have favored the epitaxial growth of urchins. Interestingly, comparative experiments carried out on γ -alumina Accu®spheres (*St-Gobain*) led to the same epitaxial growth of urchin-like MIL-53(Al) crystals (Figure S4). The amorphous nature of the ALD-alumina layer as well as the SiC support are therefore not responsible for both the formation of urchin-like crystals and epitaxial growth.

Yanai et al.²⁵ demonstrated the feasibility of aligning ZIF-8 crystals under an imposed electric field. Similarly, when MW-heating is applied, samples are also exposed to the electric component of MW irradiation. Indeed, during the oxide-to-MOF conversion, the coordinated aluminum-terephthalic acid (Al-TA) complexes and water molecules are sensitive to the orientation of the electric field. Given their high dielectric constant (ϵ') (Table S1)¹³ and dipolar characteristics, they orient themselves based on the applied electric field (Fig. 3a). Laybourn et al.¹³ have demonstrated that the dielectric properties of Al^{3+} and water are strongly affected by the concentration of Al-substrate and applied temperature. In short, when the concentration of Al(III)-salt is low (i.e. around 5 mM)

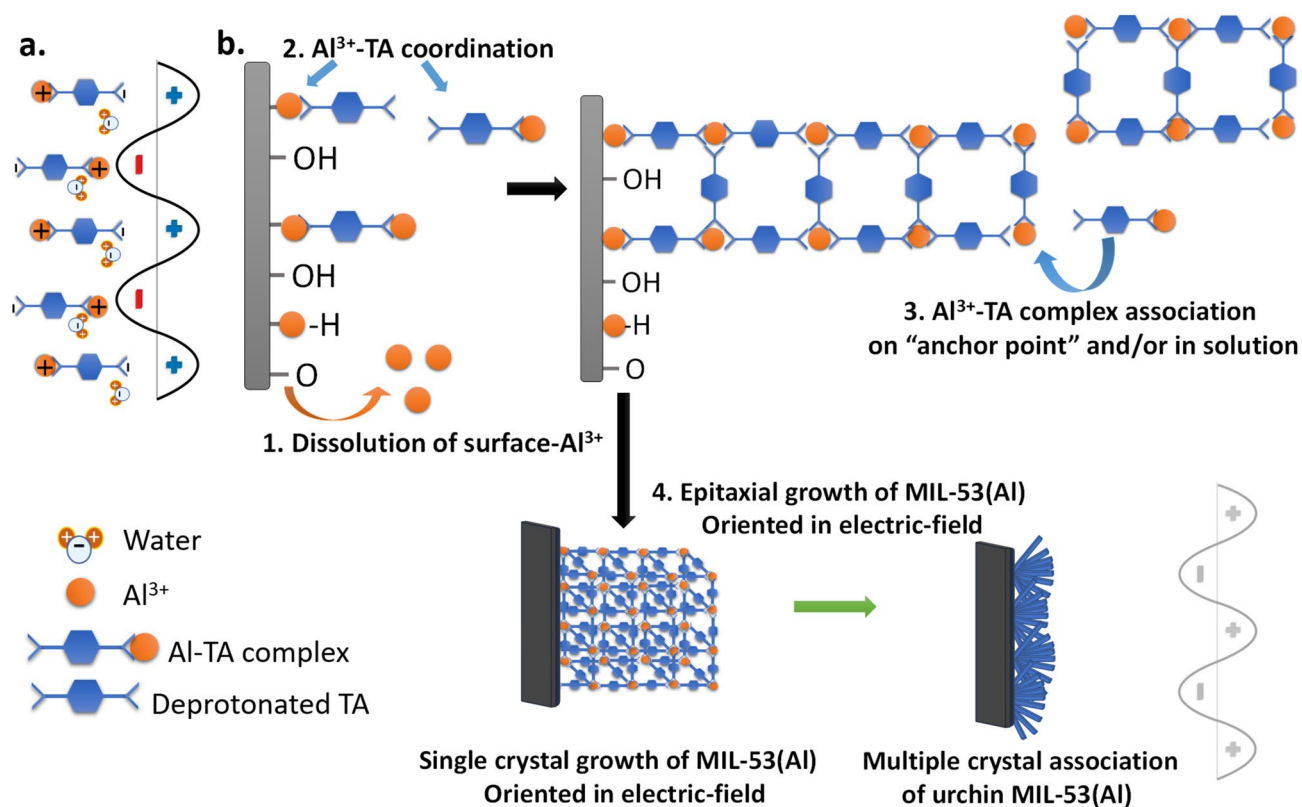


Fig. 3. (a) Orientation of Al-TA complexes and water molecules in an electric field. (b) Schematic representation of the proposed mechanism for the formation of urchin-like MIL-53(Al) crystals on a ceramic support coated with ALD-alumina, by reaction with the TA ligand in water and under MW irradiation. (The electric field is present at all stages).

the dielectric properties of Al^{3+} are dominated by those of water, but at higher Al(III) -salt concentrations (i.e. 500 mM) the effect is opposite. If the total amount of ALD- Al_2O_3 (i.e. 4 wt% determined by EDX) was accessible for MOF conversion, the reaction solution would have a maximum alumina concentration of 10 mM—a value closer to the range in which dielectric properties of water are the main parameter governing the reaction mechanism. As a result, it seems plausible that the water molecules are aligned with the applied electric field under MW irradiation and likely do orient also the Al-TA complexes. Yet, at the solid/liquid interface, a gradient of concentration does exist. Herein, it is most likely that many point areas are present on the surface, generating hotspots due to the increased dielectric loss of Al-ions at higher concentrations. Those hotspots could potentially promote coordination and nucleation on the surface of supported alumina layers, forming so-called “anchor points”.

In addition, by simply forming a metal–ligand complex with Al^{3+} (Table S1), ϵ' increases from 2.53 to 70¹³. As a result, Al-TA complexes in solution and when grafted to the anchor sites on Al_2O_3 coating, are oscillating with the electric field. Hence, we hypothesize that dissolved Al-TA complexes or pre-organized nuclei are assembled along the direction of the electric field, inducing the formation of bundled fibers with a rectangular cross-section. At this stage it is expected that MW irradiation induces an abundance of closely spaced anchor points and an excess of Al^{3+} ions or Al-TA complexes in the aqueous solution. This rapid accumulation of species could lead to steric effects at the anchor points, resulting in the formation of urchin-like structures. Contrary, without these steric effects, parallelly, ordered fibers would have been formed on the substrates. The proposed mechanism is illustrated schematically in Fig. 3b.

Potential applications of the designed materials

As mentioned in the introduction, the as-synthesized supported materials could be used in many fields such as adsorption, filtration or catalysis. In all cases, good adhesion of the MOF to the support and high mechanical stability of the system are crucial. Sonication tests carried out in ethanol with MIL-53@SiC clearly validated the stability of the sample and the excellent adhesion of crystals to the support in the tested sonication conditions. Indeed, SEM observations confirmed the preservation of urchin-like crystals on SiC foams (Figure S7). Furthermore, EDX analysis proved that the aluminum loss was very low (~0.4 wt%) even during extended sonication treatments (Table S3), therefore confirming the system's stability and the good adhesion of MOF crystals to the SiC substrate.

Attractively, the proposed synthesis approach can be applied to other ceramic supports such as ZrO_2 (Figure S8). It is however important to note that a much smaller quantity of MIL-53(Al) crystals was grown on the ZrO_2 support which is quasi-inert to MW irradiation ($\epsilon'' \sim 0.02$ and 28 for ZrO_2 and SiC, respectively). Therefore, a weight increase of only 1.1 wt% was measured for the ZrO_2 support while it reached 9.1 wt% for SiC (Table S4).

The presented synthesis method can also be exploited for the preparation of original catalyst carriers with high specific surface areas, by calcining the final ceramic supported MOF material. The concept is applicable to a wide range of ceramic supports, with special interest for MW-absorptive substrates such as SiC-based ceramics. SiC offers attractive physicochemical properties (chemical inertness, thermal conductivity, mechanical stability, magnetic, semiconductor, optical and electronic properties)²⁶, but the low specific surface area limits its use as catalytic carrier. In order to overcome this issue, MIL-53(Al) urchin-like crystals synthesized in this work could be further advantageously transformed into hierarchical nano-structured porous alumina via calcination. As demonstrated in Fig. 4, Table S4 and Figure S9, calcination of MIL-53@SiC at 1000 °C leads to the formation of a major θ - Al_2O_3 phase with a specific surface area of ~227 m²/g. Obtaining remarkably high S_{BET} values at high calcination temperatures opens the possibility to advantageously exploit these materials for the dispersion of active species (e.g. metal nanoparticles, transition metal dichalcogenides, etc.), yielding novel heterogeneous catalysts. At the same time, the high thermal and mechanical stability of the as-synthesized θ -alumina and its SiC support endows the composite material with robustness relevant for a variety of multiphase reactions conducted under harsh conditions (i.e. high pressure and temperature). Finally, preserving the urchin-like structure could strongly improve the contact of the active surface with reactants.

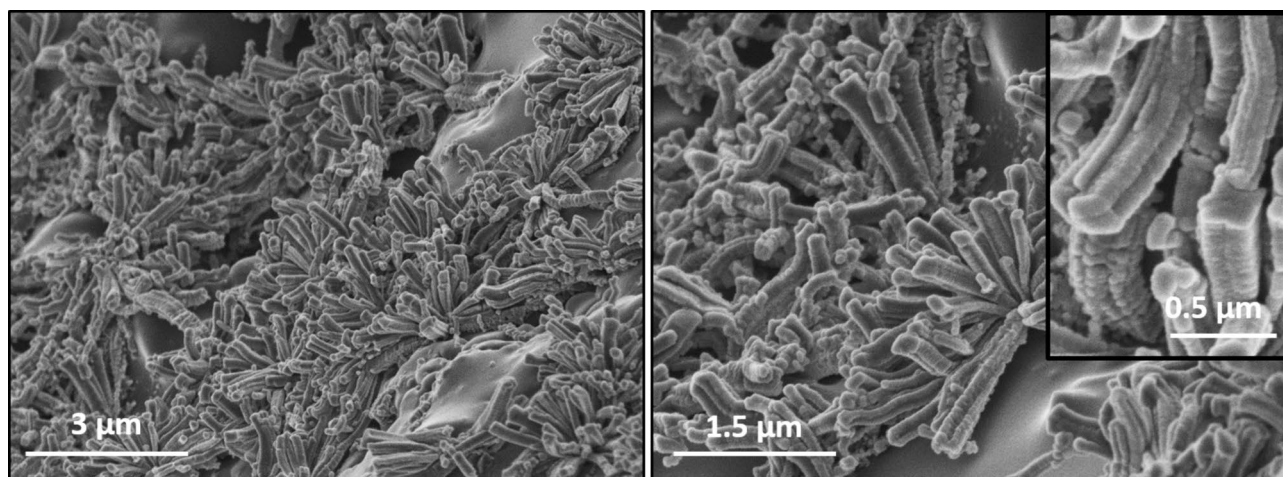


Fig. 4. SEM images of Al_2O_3 fibers obtained on SiC support after calcination of MIL-53@SiC at 1000 °C in air.

Conclusion

In this work, we have developed a robust, green and economical synthesis strategy to orient the growth of MIL-53(Al) crystals uniformly covering the accessible surface of industrial ceramic supports. This strategy leads to an increase of supports' specific surface area, which could be advantageously exploited for the design of active adsorbents or catalytic carriers. Starting from ceramic foams uniformly coated with Al₂O₃ by ALD, the MW-assisted hydrothermal reaction of the ALD-Al₂O₃ thin layers in the presence of terephthalic acid results in the formation of large, long, oriented and well-ordered MIL-53(Al) urchin-like crystals homogeneously covering the surface of ceramic substrates.

Results suggest that the epitaxial growth of large MIL-53(Al) crystals is induced by the electric-field applied during MW-assisted heating. Additionally, it has been demonstrated that ceramic supports with high dielectric losses (e.g. SiC) enable significant heat dissipation, which activates the reaction at the solid/liquid interface, thus generating a high number of nucleation sites and uniform growth of MOF crystals. The homogeneity and the quantity of crystals obtained under the proposed synthesis conditions guarantee an excellent coverage rate of the SiC support with very good adhesion.

It is assumed that the formation mechanism of urchin-type crystals is induced by a coupling of chemical reactions (i.e. oxide surface dissolution, crystal germination/growth, competition between crystal growth and re-dissolution, etc.) with specific physical phenomena occurring under MW irradiation (i.e. orientation of species in electromagnetic field, thermal gradients at interfaces, etc.). An in-depth computational study is now envisaged to further elucidate the complex growth mechanisms of MOF crystals on ceramic substrates by the oxide-to-MOF conversion strategy under MW irradiation. This type of study will be the next step forward in obtaining diverse in-situ grown MOF crystals with perfectly controlled morphology on various supports.

From an economic and ecological point of view, the combination of ALD and MW-assisted heating makes this process also attractive, since the reaction is very short and can be carried out in the absence of organic solvents. Thus, the proposed synthesis protocol generates less waste, avoids the utilization of metal-salts and reduces energy consumption. Advantageously, the as-prepared supported MIL-53(Al) can be used as an adsorbent, a catalyst or even as a template for the generation of nanostructured alumina fibers by calcination. The latter material can be used, for instance, as a catalyst carrier for bi-phasic or three-phasic reactions. Furthermore, the proposed synthesis strategy could also be applied to other ceramic substrates and with different families of MOFs, eventually converted into original nano-structured metal oxide supported materials. These original materials could reveal useful in a variety of industrial applications, ranging from selective adsorbents to sensors, including electrodes and catalytic membrane contactors.

Data availability

All data generated or analyzed during this study are included in this published article and its Supplementary Information file.

Received: 10 May 2024; Accepted: 26 August 2024

Published online: 29 August 2024

References

- Ma, Q., Zhang, T. & Wang, B. Shaping of metal-organic frameworks, a critical step toward industrial applications. *Matter* **5**, 1070–1091 (2022).
- Tomar, S. & Singh, V. K. Review on synthesis and application of mil-53. *Mater. Today Proc.* **43**, 3291–3296 (2021).
- Pereira, A., Ferreira, A. F. P., Rodrigues, A., Ribeiro, A. M. & Regufe, M. J. Shaping of ZIF-8 and MIL-53(Al) adsorbents for CH₄/N₂ separation. *Microporous Mesoporous Mater.* **331**, 1 (2022).
- Rehman, T. U. *et al.* Unveiling the MIL-53 (Al) MOF: Tuning photoluminescence and structural properties via volatile organic compounds interactions. *Nanomaterials* **14**, 1 (2024).
- Ruan, H. *et al.* Fabrication of a mil-53(al) nanocomposite membrane and potential application in desalination of dye solutions. *Ind. Eng. Chem. Res.* **55**, 12099–12110 (2016).
- Zornoza, B., Tellez, C., Coronas, J., Gascon, J. & Kapteijn, F. Metal organic framework based mixed matrix membranes: An increasingly important field of research with a large application potential. *Microporous Mesoporous Mater.* **166**, 67–78 (2013).
- Linares-Moreau, M. *et al.* Fabrication of oriented polycrystalline MOF superstructures. *Adv. Mater.* **36**, 1 (2024).
- Amirilargani, M. *et al.* MIL-53(Al) and NH₂-MIL-53(Al) modified α -alumina membranes for efficient adsorption of dyes from organic solvents. *Chem. Commun.* **55**, 4119–4122 (2019).
- Wang, Y., Ban, Y., Hu, Z. & Yang, W. Template Triggers the Formation of a Highly Compact MIL-53 Metal-Organic Framework. *Angew. Chemie Int. Ed.* **62**, 16 (2023).
- Klinowski, J., Almeida Paz, F. A., Silva, P. & Rocha, J. Microwave-assisted synthesis of metal-organic frameworks. *Dalt. Trans.* **40**, 321–330 (2011).
- Usman, K. A. S. *et al.* Downsizing metal–Organic frameworks by bottom-up and top-down methods. *NPG Asia Mater.* **12**, 1 (2020).
- Gawande, M. B., Shelke, S. N., Zboril, R. & Varma, R. S. Microwave-assisted chemistry: Synthetic applications for rapid assembly of nanomaterials and organics. *Acc. Chem. Res.* **47**, 1338–1348 (2014).
- Laybourn, A. *et al.* Understanding the electromagnetic interaction of metal organic framework reactants in aqueous solution at microwave frequencies. *Phys. Chem. Chem. Phys.* **18**, 5419–5431 (2016).
- Samanta, S. K., Basak, T. & Sengupta, B. Theoretical analysis on microwave heating of oil-water emulsions supported on ceramic, metallic or composite plates. *Int. J. Heat Mass Transf.* **51**, 6136–6156 (2008).
- Ji, T. *et al.* Intense microwave heating at strongly polarized solid acid/water interface for energy-efficient platform chemical production. *Chem. Eng. Sci.* **262**, 118035 (2022).
- Drobek, M. *et al.* An innovative approach for the preparation of confined ZIF-8 membranes by conversion of ZnO ALD layers. *J. Memb. Sci.* **475**, 39–46 (2015).
- Drobek, M. *et al.* MOF-based membrane encapsulated ZnO nanowires for enhanced gas sensor selectivity. *ACS Appl. Mater. Interfaces* **8**, 8323–8328 (2016).
- Bechelany, M. *et al.* Highly crystalline MOF-based materials grown on electrospun nanofibers. *Nanoscale* **7**, 5794–5802 (2015).

19. Liu, Y., Liu, S. & Yue, Z. Mesoporous alumina nanosheets and nanorolls derived from topologically identical Al-based MOFs. *RSC Adv.* **5**, 31742–31745 (2015).
20. Heni, W., Vonna, L. & Fioux, P. Ultrasonic cavitation test applied to thin metallic films for assessing their adhesion with mercaptosilanes and surface roughness. *J. Mater. Sci.* **49**, 6750–6761. <https://doi.org/10.1007/s10853-014-8369-y> (2014).
21. Lian, H. *et al.* Highly durable ZIF-8 tubular membranes via precursor-assisted processing for propylene / propane separation. *J. Memb. Sci.* **660**, 120813 (2022).
22. Yi, M. *et al.* Surface-enhanced raman scattering activity of zno2 nanoparticles: Effect of tetragonal and monoclinic phases. *Nanomaterials* **11**, 2162 (2021).
23. Biscay, N., Henry, L., Adschiri, T., Yoshimura, M. & Aymonier, C. Behavior of silicon carbide materials under dry to hydrothermal conditions. *Nanomaterials* **11**, 1 (2021).
24. Kim, J., Lee, S., Kim, J. & Lee, D. Metal-organic frameworks derived from zero-valent metal substrates: Mechanisms of formation and modulation of properties. *Adv. Funct. Mater.* **29**, 1 (2019).
25. Yanai, N., Sindoro, M., Yan, J. & Granick, S. Electric field-induced assembly of monodisperse polyhedral metal-organic framework crystals. *J. Am. Chem. Soc.* **135**, 34–37 (2013).
26. Xu, M. *et al.* Recent advances and challenges in silicon carbide (SiC) ceramic nanoarchitectures and their applications. *Mater. Today Commun.* **28**, 102533 (2021).

Acknowledgements

This research was funded by the French National Research Agency (ANR project PEHY-0016-BHYOLOHC). The authors also acknowledge Saint-Gobain NorPro for providing alumina-Accu[®]spheres.

Author contributions

A.J. and L.B.N. conceived the research strategy and analysed results, L.B.N. and M.D. conducted MOF synthesis and characterisation, M.B. conceived and optimized the ALD protocol, L.B.N. and B.R. conducted EDX-SEM analysis, L.B.N. wrote the first draft and all co-authors reviewed the final manuscript.

Competing interests

The authors declare no competing interests.

Additional information

Supplementary Information The online version contains supplementary material available at <https://doi.org/10.1038/s41598-024-71150-7>.

Correspondence and requests for materials should be addressed to A.J.

Reprints and permissions information is available at www.nature.com/reprints.

Publisher's note Springer Nature remains neutral with regard to jurisdictional claims in published maps and institutional affiliations.

Open Access This article is licensed under a Creative Commons Attribution-NonCommercial-NoDerivatives 4.0 International License, which permits any non-commercial use, sharing, distribution and reproduction in any medium or format, as long as you give appropriate credit to the original author(s) and the source, provide a link to the Creative Commons licence, and indicate if you modified the licensed material. You do not have permission under this licence to share adapted material derived from this article or parts of it. The images or other third party material in this article are included in the article's Creative Commons licence, unless indicated otherwise in a credit line to the material. If material is not included in the article's Creative Commons licence and your intended use is not permitted by statutory regulation or exceeds the permitted use, you will need to obtain permission directly from the copyright holder. To view a copy of this licence, visit <http://creativecommons.org/licenses/by-nc-nd/4.0/>.

© The Author(s) 2024